SLEEPJ, 2022, 1–13

https://doi.org/10.1093/sleep/zsac062
Advance Access Publication Date: 13 March 2022
Original Article

ORIGINAL ARTICLE

Sleep–wake states change the interictal localization of candidate epileptic source generators

Graham A. McLeod[1,*], Parandoush Abbasian[2,3], Darion Toutant[4], Amirhossein Ghassemi[4], Tyler Duke[4], Conrad Rycyk[4], Demitre Serletis[5,6], Zahra Moussavi[4] and Marcus C. Ng[4,7]

[1]Department of Clinical Neurosciences, University of Calgary, Calgary, AB, Canada, [2]Medical Physics, Department of Physics and Astronomy, University of Manitoba, Winnipeg, MB, Canada, [3]CancerCare Manitoba Research Institute, Winnipeg, MB, Canada, [4]Biomedical Engineering, University of Manitoba, Winnipeg, MB, Canada, [5]Charles Shor Epilepsy Center, Cleveland Clinic, Cleveland, OH, USA, [6]Department of Neurosurgery, Cleveland Clinic Foundation, Cleveland, OH, USA and [7]Section of Neurology, University of Manitoba, Winnipeg, MB, Canada

*Corresponding author. Graham A. McLeod, Section of Neurology, Department of Clinical Neurosciences, University of Calgary, 1403 29 Street NW, Calgary, AB T2N 2T9, Canada. Email: graham.mcleod@ucalgary.ca.

Abstract

Study Objectives: To compare estimated epileptic source localizations from 5 sleep–wake states (SWS): wakefulness (W), rapid eye movement sleep (REM), and non-REM 1-3.

Methods: Electrical source localization (sLORETA) of interictal spikes from different SWS on surface EEG from the epilepsy monitoring unit at spike peak and take-off, with results mapped to individual brain models for 75% of patients. Concordance was defined as source localization voxels shared between 2 and 5 SWS, and discordance as those unique to 1 SWS against 1–4 other SWS.

Results: 563 spikes from 16 prospectively recruited focal epilepsy patients across 161 day-nights. SWS exerted significant differences at spike peak but not take-off. Source localization size did not vary between SWS. REM localizations were smaller in multifocal than unifocal patients (28.8% vs. 54.4%, $p = .0091$). All five SWS contributed about 45% of their localizations to converge onto 17.0 ± 15.5% voxels. Against any one other SWS, REM was least concordant (54.4% vs. 66.9%, $p = .0006$) and most discordant (39.3% vs. 29.6%, $p = .0008$). REM also yielded the most unique localizations (20.0% vs. 8.6%, $p = .0059$).

Conclusions: REM was best suited to identify candidate epileptic sources. sLORETA proposes a model in which an "omni-concordant core" of source localizations shared by all five SWS is surrounded by a "penumbra" of source localizations shared by some but not all SWS. Uniquely, REM spares this core to "move" source voxels from the penumbra to unique cortex not localized by other SWS. This may reflect differential intra-spike propagation in REM, which may account for its reported superior localizing abilities.

Statement of Significance

To treat epilepsy, it is important to locate the brain region responsible for generating seizures. This requires understanding how seizures spread within the brain. Sleep is a well-known activator and de-activator of seizures, but the effects of specific sleep–wake states on epileptic cortex remain poorly defined in spatial dimensions. Using electrical source localization, we found sleep–wake states within any single given patient brain partially agree, and dynamically disagree, about which cortical areas generate seizures. In particular, the effects of REM sleep differ from those of all other sleep–wake states. These findings extend present knowledge of the profound impacts of sleep on localization in epilepsy, and provide a possible mechanism for REM's reportedly superior localizing ability out of all SWS.

Submitted: 23 May, 2021; **Revised:** 28 February, 2022

Key words: rapid eye movement sleep; sleep activation; sleep wake states; epilepsy; seizures; epileptic generator; source localization; source generator; sLORETA; concordance

Introduction

Sleep and epilepsy are both phenomena generated by the brain, with interdependent effects and interactions. Sleep, as essential to survival as food and oxygen, is a recurrent physiological change with profound and immediate effects on the brain's electrodynamics, as measured by EEG. Far from a dormant state, sleep is a highly choreographed nightly cerebral symphony that activates or inhibits epileptic activity. Epilepsy is defined as the predisposition to recurring unprovoked seizures, which are pathological paroxysms of hyperexcitable and often hypersynchronous electrical brain activity. Every 3.5 min, a new case of epilepsy is diagnosed in the USA [1]. Studying how different sleep–wake states (SWS) impact epileptic source generators offers new insights into the treatment of a common, serious cause of neurological disability worldwide [2].

For epilepsy patients, eliminating seizures reduces the risk of premature death [3], adverse cognitive sequelae [4], and other somatic health detriments due to epilepsy [1]. In the 30%–40% of epilepsy refractory to antiseizure medications [5, 6], surgically resecting the epileptic generator becomes the most effective and economical treatment [7, 8]. However, resection requires carefully locating the generator to spare nonoffending eloquent regions [9]. Difficulty triangulating the generator contributes to the approximately half of well-selected resective surgery patients who do not achieve postsurgical seizure freedom [10], despite a comprehensive presurgical evaluation.

In recent years, there have been growing reports of enhanced EEG localization of the generator when interictal epileptiform activity occurs in sleep [11–15]. Instead of simply inferring localization of the epileptic generator from passive recordings of topographical EEG voltage fields, electrical source localization (ESL) techniques actively solve the inverse problem [16] by calculating probabilistic source localization estimates of the epileptic generator for observed EEG activity [17]. ESL estimates of the source generator can be reliably obtained from surface interictal EEG activity, and typically reliably localize with the epileptogenic zone (EZ) [18–20] as validated by postoperative seizure freedom [18, 19]. Therefore, interictal ESL techniques are increasingly routine in presurgical evaluation to guide the neurosurgical implantation of intracranial electrodes [16]. However, despite awareness since at least the 1940s [21] of complex interactions between epileptic cortex and different SWS, the effects of SWS on interictal ESL have been scarcely considered to date [22, 23].

In this study, we applied ESL to interictal epileptiform activity (for convenience, "spikes") to compare the relative source localizations of the five canonical SWS: wakefulness (W), rapid eye movement sleep (REM), non-REM stage 1 (N1), non-REM stage 2 (N2), non-REM stage 3 (N3). Spikes were analyzed at their peak, and in the early phase shortly after onset ("take-off"). Within individual brains of prospectively recruited focal epilepsy patients, we quantify the size, spatial overlap ("concordance"), and nonoverlap ("discordance") of source localizations derived from interictal spikes in each SWS.

Methods

Subjects and subgroups

The Institutional Research Ethics Board approved this study. Focal epilepsy patients were prospectively recruited from the epilepsy monitoring unit (EMU) at the University of Manitoba Health Sciences Centre from October 2017 to April 2019. Exclusion criteria were (1) age under 18 years, and (2) diagnosis of generalized epilepsy. Inclusion criteria were spikes in all five canonical SWS (N1, N2, N3, wakefulness, REM). We delineated "multifocal" and "unifocal" subgroups based on retrospective chart review of semiology, neurological examination, ictal and interictal EEG in EMU, neuroimaging, neuropsychological testing, and the resultant clinically posited seizure onset zone(s).

EEG acquisition and preprocessing

Surface EEG was sampled at 500 Hz using 25 electrodes per the International 10–20 system including additional extended bilateral subtemporal chains, processed using bandpass filters with respective low and high frequencies of 1 and 70 Hz, and a 60 Hz notch filter. EEG data were visually reviewed in bipolar longitudinal, transverse, and referential montages at a time base of 30 mm/s in Neuroworks 7.1 software (Natus, Oakville, Canada).

Individualized brain models

Using recent individual clinical brain MRIs, we applied the boundary-element method (BEM [24]) to generate individual realistic volume conductor head models for co-localizing spike source current density reconstructions by ESL (Figure 1C). BEM head models provide a personalized anatomical substrate for source localization, allowing greater accuracy than when standard templates are used [25]. For patients who have undergone prior epileptic resective surgery, BEM can account for resection cavities without significant decrease in source localization accuracy [26]. BEM head models yielded a list of individualized cortical grey matter voxels (arrayed in personalized 3D brain space) and were visually confirmed for clinical congruence. If recent clinical imaging was unavailable, standard cortex templates were substituted.

Spike inclusion and SWS assignment

As part of routine clinical care, EEGs had already been annotated for spikes. Where spikes occurred in repetitive runs, only the most noteworthy instances had been typically annotated. A board-certified epileptologist (M.C.N.) included these flagged spikes if visually confirmed as free of artifact and meeting accepted epileptiform discharge criteria [27]. When no spikes had been annotated in an SWS, we simulated clinical care to annotate additional spikes if possible, with reconfirmation (M.C.N.). Thus, spike counts are not a true measure of spike frequency per SWS.

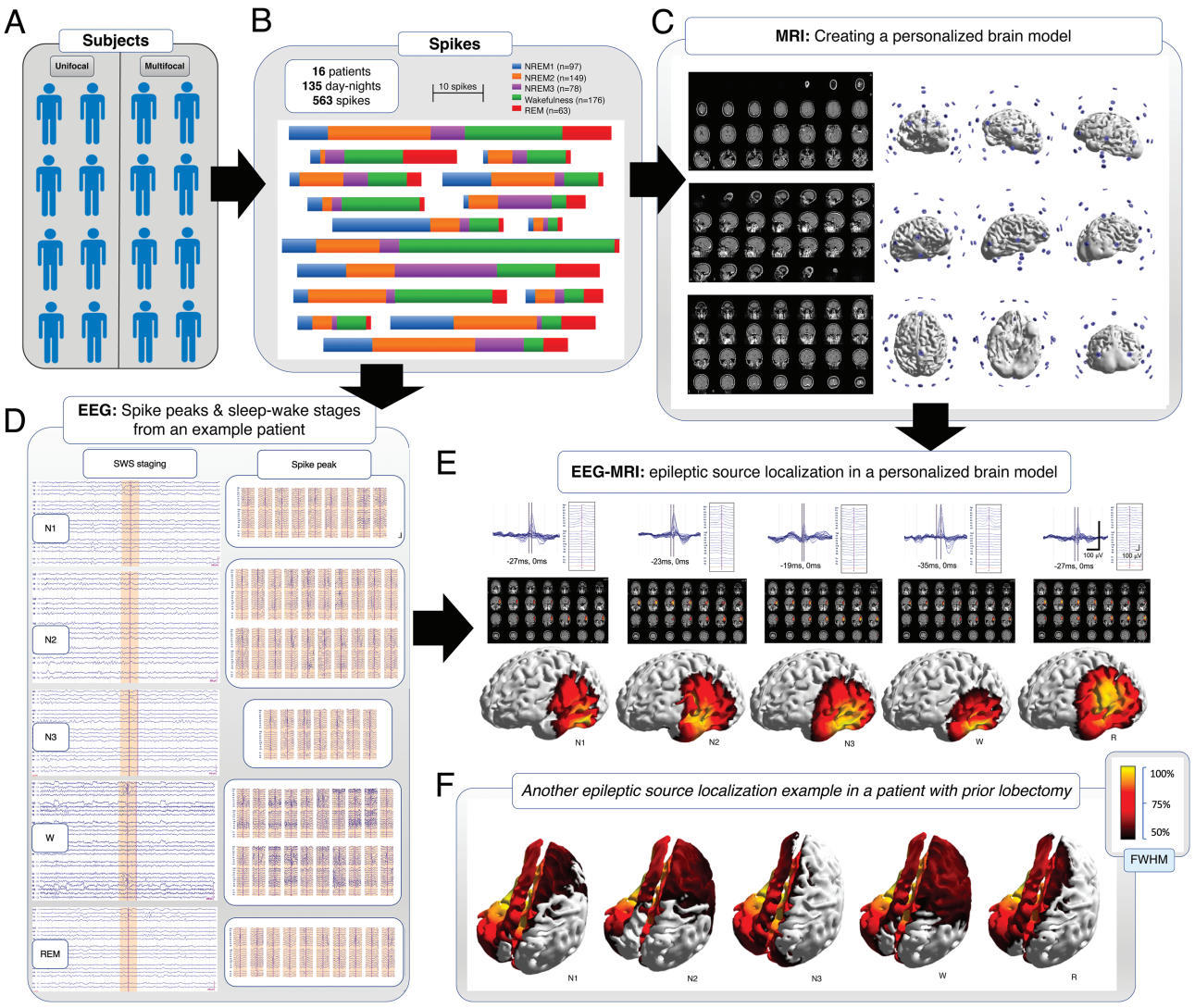

Figure 1. Source localization pipeline. (A) 16 prospectively recruited focal epilepsy patients met inclusion criteria of having spikes in all five canonical SWS. Patients subdivided equally into eight with unifocal epilepsy and eight with multifocal epilepsy. (B) Schematic subdivision of 563 spikes over five different SWS. Subjects are separated by gaps. Bar length is proportional to number of spikes. Different colors represent different SWS. (C) Personalized 3D brain model generated from MRI data. Axial, sagittal, and coronal T1 MR images shown. Electrodes shown in position relative to brain model. (D) Spike identification and peak selection (example referential montage) and SWS staging (example bipolar montage) in an example patient. (E) Butterfly plots showing SWS spike overlays, SWS composite spikes in EEG average referential montage, and sLORETA source localizations (colored region) from spike peak in an example patient (patient 2). Source localizations for a given SWS were defined as the aggregate of all cortical grey matter voxels containing a plausible epileptic source generator as determined by full-width half-maximum (FWHM) thresholding (scale begins at 50%). (F) Example of source localizations from spike peak within realistic brain modelling in another patient (patient 3) who underwent prior resective epilepsy surgery.

Pre-ESL spike processing

All included spikes were transferred for ESL into Curry 8 software (Compumedics, Abbotsford, Australia), and marked at spike peak and take-off (G.A.M., P.A., A.G., T.D., C.R.). Like others [28, 29], we defined spike take-off as the "first clear disruption of background rhythm that reached >50% amplitude of preceding baseline activity", which was visually estimated. Following spike transfer into ESL software, a board-certified epileptologist (M.C.N.) assigned a SWS to each spike by applying American Academy of Sleep Medicine sleep scoring criteria (modified without chin electromyography) based on the antecedent and subsequent 15 s of EEG [30]. All spikes in a single SWS were averaged into one composite spike representing that SWS in a patient (Figure 1D) [31].

ESL and thresholding

We conducted a separate ESL for spike take-off and a separate ESL for spike peak. We performed all ESL on composite spikes via source current density reconstruction by standardized low resolution electromagnetic tomography analysis (sLORETA). Based upon a linear sum of surface-recorded EEG potentials, sLORETA assigns each individualized cortical grey matter voxel a probability of a source current dipole moment by calculating a pseudo-*f*-statistic of current density variance between noise (technical and biological) and signal (the spike) per voxel [32]. We adopted standard convention of full-width-at-half-maximum (FWHM) thresholding of the pseudo-*f*-statistic to binarize voxels above threshold as those demonstrating presence of a plausible source localization; in other words, a voxel "activation"

[30,33,34]. The collection of activated cortical grey matter voxels above FWHM threshold represented the source localizations given by that SWS in that patient (Figure 1E,F).

Intraindividual source localization concordances

We defined concordance as spatial overlap/agreement of SWS source localizations within a patient, represented by the mathematical intersection "∩" [23]. We defined a five-way "omniconcordance" as the voxels activated unanimously by all five canonical SWS: "N1∩N2∩N3∩W∩REM". We also defined two--way "head-to-head" concordance as the voxels activated together by two SWS ("$SWS_1 \cap SWS_2$"), irrespective of other SWS in that patient. All concordances were expressed as a fraction of total individualized cortical grey matter voxels. Five-way omniconcordance was also expressed as a fraction of the source localizations from each SWS. Two-way concordances were also expressed relative to the sum of the two SWS source localizations, "$(2)(SWS_1 \cap SWS_2)/(SWS_1 + SWS_2)$", akin to the Jaccard index [35].

Intraindividual source localization discordances

We defined discordance as spatial nonoverlap disagreement between SWS source localizations within a patient, represented by a mathematical null intersection "∩= Ø" [23]. We defined a five-way "absolute discordance" as voxels uniquely activated by only one SWS but none of the four other SWS: "$SWS_1 \cap x = Ø$; $x = SWS_{2\text{-}5}$". We defined a two-way "head-to-head" discordance between any two SWS as voxels activated by SWS_1 but not SWS_2: "$SWS_1 \cap SWS_2 = Ø$". We pooled two-way discordances by SWS_1 for analysis. In the example of SWS_1 = W, pooled two-way discordances are "W∩N1 = Ø", "W∩N2 = Ø", "W∩N3 = Ø", and "W∩REM = Ø". Discordances were expressed as a fractions of total individualized cortical grey matter voxels or SWS_1 source localizations.

Statistical tests

Normality was assessed using the Shapiro–Wilks test. We assessed all source localization size, concordance, and discordance comparisons between SWS using one-way ANOVA if parametric, and the Kruskal–Wallis test if nonparametric. Multifocal vs. unifocal source localization size was assessed via Student's *t*-test if parametric and the Wilcoxon rank sum test if nonparametric. We assessed correlations between spike count against source localization size, concordance, and discordance using Pearson's test if parametric, and Spearman's test if nonparametric. We applied Benjamini–Hochberg significance correction of *p*-values against a $p = 0.05$ statistical significance threshold for multiple correlations. All statistics were conducted with Stata 14 software (StataCorp, TX, USA).

Results

Patients, spikes, and source localizations

From 50 prospectively and sequentially recruited EMU patients, 16 met inclusion criteria of focal epilepsy with spikes in all five SWS during EMU admission (mean 5–20 days, range 10.1; Table 1). Of these patients, eight were clinically unifocal, eight were clinically multifocal. Mean patient age was 38 years. 9/16 were female. Most patients had unilateral or bilateral temporal lobe epilepsy (11/16) and were on three antiseizure medications (mean = 2.73, mode = 3), most commonly lamotrigine (11/16). Two patients underwent resective surgery (Engel II and III), and one underwent disconnective surgery (Engel I), after EMU admission. From a total of 161 day-night EEG recordings, 135 day-nights yielded 563 spikes for analysis (Figure 1A). We achieved individual realistic brain modeling with clinical MRI (Figure 1C) in 12/16 patients (range 11 397–21 831 voxels vs. standardized 18141 in 4/16 patients). We analyzed a total of 80 composite spikes, one representing each of 5 SWS in each of 16 patients.

Source localization size differs not by sleep–wake state, but by focality

Amongst $n = 16$, source localization size did not significantly differ by SWS at spike peak (one-way ANOVA $p = .9763$; % cortical grey matter, range of means: wakefulness 41.3% to NREM1 44.7%; Figure 2B) nor take-off (Kruskal–Wallis $p = .6578$; % cortical grey matter, range of means: REM 59.8% to NREM3 66.3%). At spike peak and take-off, source localization size also did not differ by SWS amongst $n = 8$ unifocal patients (peak: one-way ANOVA $p = .6401$; take-off: Kruskal–Wallis $p = .7802$), nor amongst $n = 8$ multifocal patients (peak: one-way ANOVA $p = .2222$; take-off: one-way ANOVA $p = .4144$). At spike peak, multifocal ($n = 8$) source localization sizes were overall larger than unifocal ($n = 8$) localization sizes (Student's *t*-test $p = 0.0384$, mean 46.8% vs. 38.8%). At spike take-off, there was no significant difference (Wilcoxon rank sum $p = .8399$). Comparing SWS source localizations between $n = 8$ unifocal vs. $n = 8$ multifocal patients derived from spike peaks, only REM amongst SWS exhibited a significant difference between groups, with smaller REM source localizations amongst multifocal patients (Student's *t*-test $p = .0091$; mean 28.8% vs. 54.4% cortical grey matter; Figure 2C, D). Comparing SWS source localizations between $n = 8$ unifocal vs. $n = 8$ multifocal patients derived at spike take-off, no SWS exhibited a significant size difference between groups (Student's *t*-test N1 $p = .9715$, N2 $p = .4267$, N3 $p = .4030$, W $p = .3891$, R $p = .3767$).

Source localizations from all five SWS share a core zone of spatial agreement

We evaluated how much cortical grey matter was concordantly localized by all five SWS, unanimously. We found that five SWS spatially converged onto an "omniconcordant zone" (N1∩N2∩N3∩W∩REM) spanning 17.0 ± 15.5% (spike peak; range: 0–54.0% cortical grey matter) and 24.2 ± 19.0% (spike take-off; range: 0.8–52.4% cortical grey matter) of individualized cortical grey matter voxels. Considering how much of the source localization voxels from each SWS was included in this omniconcordant zone, there was no significant difference between SWS at spike peak (Kruskal–Wallis $p = .9942$; range of means, proportion of source localizations from a SWS contributing to shared five-way concordance: N1 42.7% to N3 47.0%, global mean 45.3%; Figure 3B) nor take-off (Kruskal–Wallis $p = .8902$; range of means, proportion of source localizations from a SWS contributing to shared five-way concordance: N3 32.7% to W 40.0%, global mean 36.9%).

In % cortical grey matter at spike peak, omniconcordance was 19.4 ± 18.3% for unifocal, and 14.7 ± 13.1% for multifocal

Table 1. Patient demographics. Sex indicated as M or F (male or female), handedness as R or L (right or left)

								Spikes in SWS					
Patient ID	Demo	Multifocal	Focus	ASM	Etiology	MRI Tesla	EMU LOS	N1	N2	N3	W	R	All
1	19F R	Yes	B/l anterior	LTG	Greig syndrome	1.5	7	2	1	4	12	11	30
2	54M R		L insular	LTG, CBZ	Cavernoma	3	9	2	9	5	8	3	27
3	27F L		L hemisphere	CBZ, LTG, PER	Stroke	1.5	7	3	2	2	16	1	24
4	62F R	Yes	Bitemporal	LTG	Idiopathic	1.5	6	20	6	2	6	1	35
5	20F R		R temporal	LTG, CLB	MTS	3	7	1	2	1	2	1	7
6	34F R	Yes	L temporal & midline	VPA, CBZ, LEV	MTS	1.5	13	13	17	1	4	7	42
7	20F R		R frontal	CLB, LTG, CBZ	Stroke	N/A	5	3	4	1	6	1	15
8	54M L		R temporal	LEV, VPA, CBZ	MTS	3	9	10	13	2	7	1	33
9	74M R	Yes	Bitemporal	Nil	MTS	3	11	1	6	11	3	4	25
10	23M R	Yes	Bitemporal	VPA, LTG	Glioma	3	16	10	10	21	12	9	62
11	45F L		L frontal	CBZ, VPA, GBP	Idiopathic	N/A	8	2	4	2	4	4	16
12	26M R		L temporal	CLZ, PHT, VPA, LTG	CNS Vasculitis	3	9	10	21	10	4	5	50
13	36M R	Yes	Bitemporal	VPA, PHT, LTG, LCM	MTS	N/A	18	7	13	4	44	1	69
14	37M R	Yes	Bitemporal	LEV, GBP, LCM, TPM, CLZ	Trauma	N/A	8	3	16	2	20	3	44
15	25F R		R temporal	LTG, PHT	MTS	1.5	8	1	5	3	8	1	18
16	58F R	Yes	Bitemporal	LEV, LTG, LCM	Meningioma	3	20	9	20	7	20	10	66

ASM, anti-seizure medication; b/l, bilateral; CBZ, carbamazepine; CLB, clobazam; CLZ, clonazepam; CNS, central nervous system; demo, demographics; EMU, epilepsy monitoring unit; GBP, gabapentin; LCM, lacosamide; LEV, levetiracetam; LOS, length of stay; LTG, lamotrigine; MTS, mesial temporal sclerosis; PER, perampanel; PHT, phenytoin; TPM, topiramate; VPA, valproic acid.

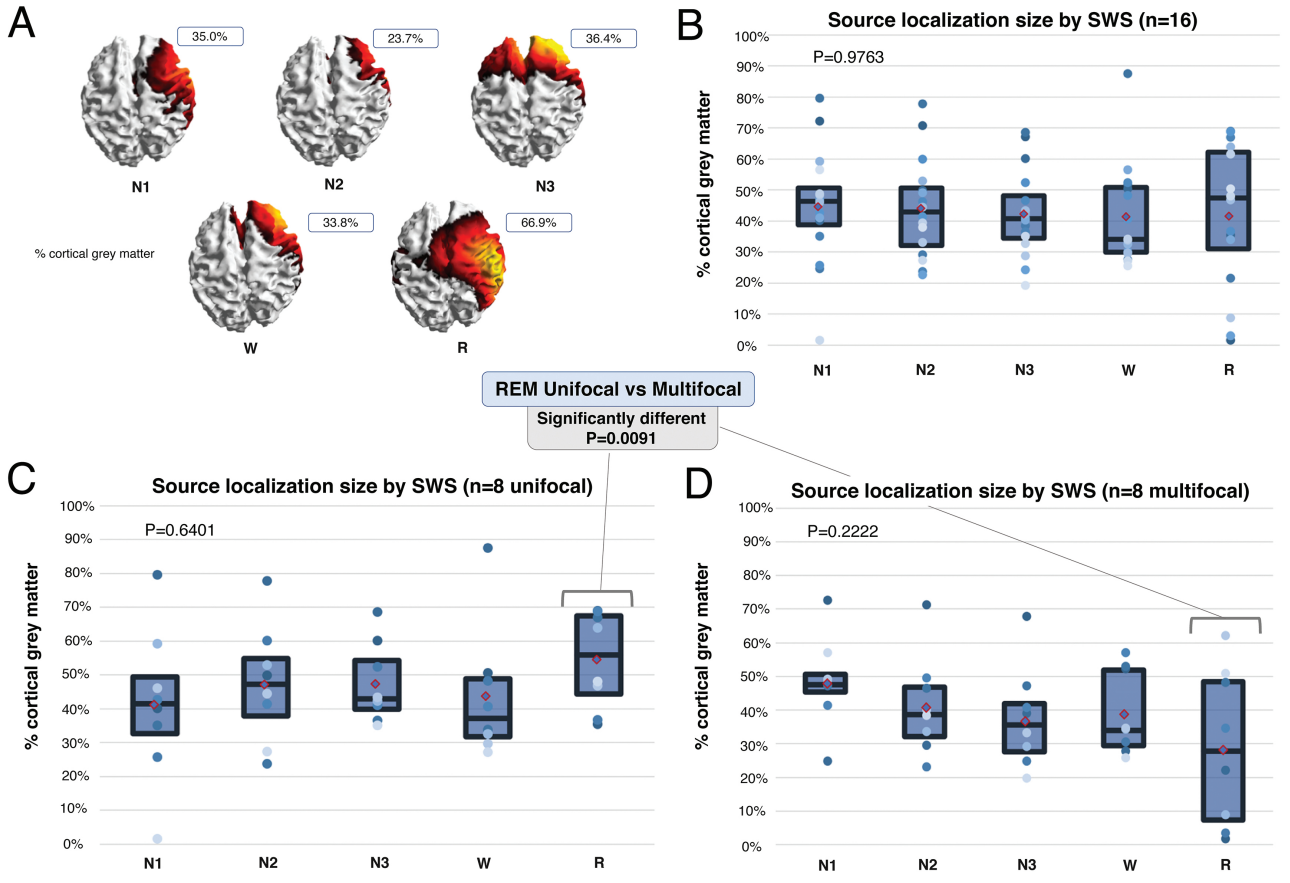

Figure 2. Source localization size at spike peak differs not by sleep–wake state, but by focality. (A) Example patient (patient 5) illustrates visual scale of source localization sizes. (B)–(D) Source localization size did not significantly vary by SWS at spike peak, but REM source localizations differed significantly between unifocal versus multifocal subgroups, with smaller REM source localizations amongst multifocal patients. Diamonds depict the mean, dots depict individual patient data points, and boxes depict median ± IQR.

subgroups. At spike take-off, omniconcordance was 28.2 ± 23.0% for unifocal, and 20.2 ± 14.5% for multifocal subgroups. Considering how much of the source localization voxels from each SWS was included in this omniconcordant zone, at spike peak, there was no significant difference between SWS in the unifocal group (Kruskal–Wallis p = .9314) nor the multifocal group (Kruskal–Wallis p = .9329), nor at spike take-off (Kruskal–Wallis unifocal p = .8859; multifocal p = .8548).

Source localizations in REM are least agreeable with any one other SWS

We also examined the spatial concordance of source localization voxels between any two SWS (instead of all five SWS at once). At spike peak and spike take-off, these two-way "head-to-head" SWS concordances did not significantly differ when taken as a fraction of a patient's individual total cortical grey matter voxels (spike peak Kruskal–Wallis p = .4215; spike take-off Kruskal–Wallis p = .7299). However, taken as a fraction of brain space occupied by the source localizations of those two SWS, head-to-head concordances significantly differed such that REM exhibited the least concordance at spike peak (Kruskal–Wallis p = .0006; range of two-way concordance means, proportion of spatial overlap between SWS_1 and SWS_2: REM∩W 53.1% to N2∩W 82.0%, global mean: SWS_1∩SWS_2 66.9%; Figure 3C). At spike take-off, concordance did not significantly differ as a fraction of the brain space occupied by those two SWS (Kruskal–Wallis p = .7370).

Delineating unifocal and multifocal subgroups at spike peak, amongst n = 8 unifocal patients, two-way concordances did not differ as a fraction of cortical grey matter (Kruskal–Wallis p = .9509) nor as a proportion of spatial overlap between the two SWS (Kruskal–Wallis p = .4385). Amongst n = 8 multifocal patients, two-way concordances significantly differed such that REM exhibited the least concordance as a fraction of cortical grey matter (Kruskal–Wallis p = .0246; range of two-way concordance means, proportion of spatial overlap between SWS_1 and SWS_2: REM∩N3 15.8% to N1∩N2 35.4%, global mean: SWS_1∩SWS_2 27.3%) and as a proportion of spatial overlap between the two SWS (Kruskal–Wallis p = .0041; range of two-way concordance means, proportion of spatial overlap between SWS_1 and SWS_2: REM∩N3 42.8% to N3∩W 84.5%, global mean: SWS_1∩SWS_2 67.5%). At spike take-off amongst unifocal and multifocal patients, two-way concordances did not differ as a fraction of cortical grey matter (Kruskal–Wallis unifocal p = .8222; multifocal p = .6128) nor as a proportion of spatial overlap between the two SWS (Kruskal–Wallis unifocal p = .9804; multifocal p = .5550).

REM source localizations are also most disagreeable with any one other SWS

Considering the spatial discordance of source localization voxels between a SWS and just one other SWS, when these individual "head-to-head" discordances were pooled by SWS and expressed as a fraction of cortical grey matter voxels, there

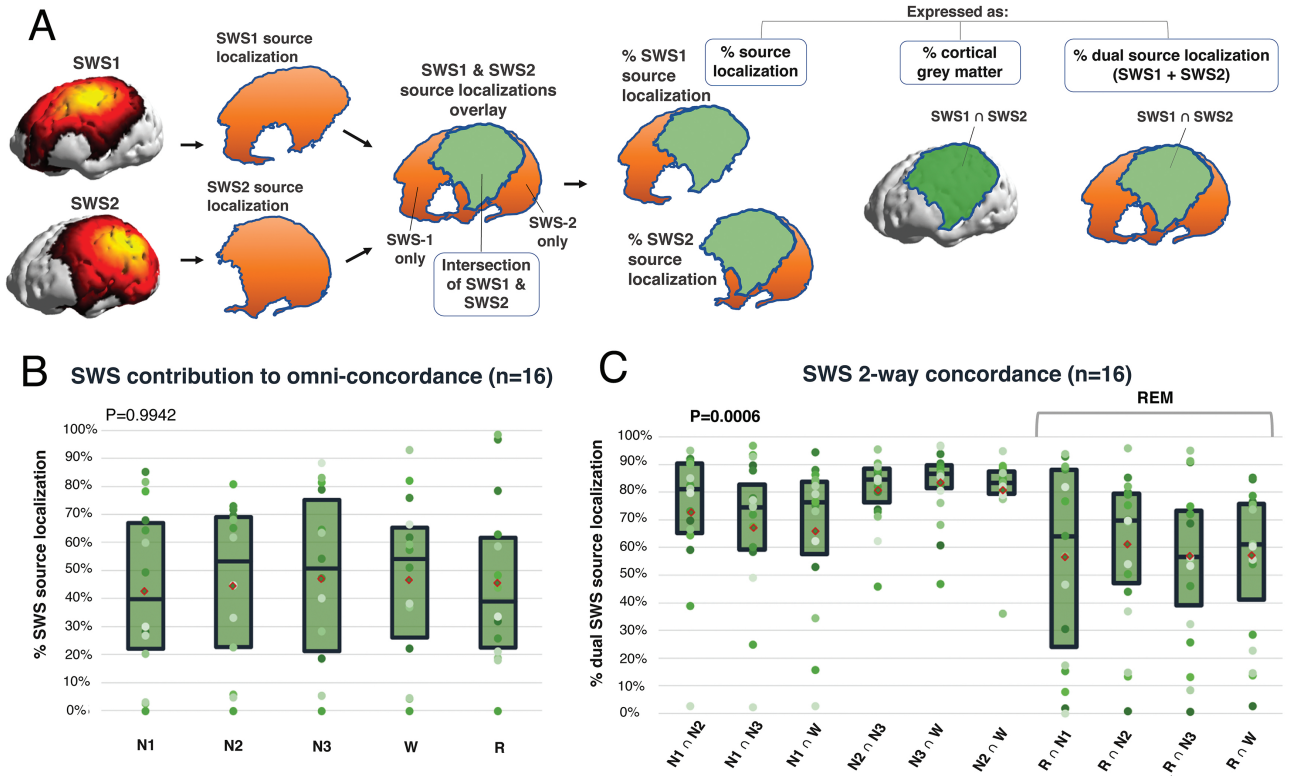

Figure 3. REM detracts from two-way SWS concordance at spike peak while retaining five-way SWS "omni"-concordance. (A) Schematic illustrating concordance of source localizations for a hypothetical SWS_1 and SWS_2, expressed as a fraction of source localizations from each SWS, total cortical grey matter voxels in that individual, and source localizations of either SWS. (B, C) Diamonds depict the mean, dots depict individual patient data points, and boxes depict median ± IQR. (B) Contribution of each SWS, as a fraction of its own source localizations, to the five-way omniconcordant region. (C) two-way concordances among as a fraction of the sum of the two SWS source localizations.

was no significant difference between SWS (Kruskal–Wallis p = .1913). However, expressing two-way discordance as a fraction of source localization size, REM was significantly the most discordant SWS (Kruskal–Wallis p = .0008; range of two-way discordance means, proportion of spatial nonoverlap between SWS_1 and SWS_2: W 23.8% to REM 39.2%, global mean 29.6%; Figure 4B). At spike take-off, two-way disconcordance did not significantly differ as a fraction of a patient's total cortical grey matter voxels (Kruskal–Wallis p = .3957) nor as a fraction of that SWS source localization size (Kruskal–Wallis p = .5698).

Delineating unifocal and multifocal subgroups at spike peak, amongst n = 8 unifocal patients, two-way discordances significantly differed, with REM most discordant in terms of % cortical grey matter (Kruskal–Wallis p = .0045; range of two-way discordance means, proportion of spatial nonoverlap between SWS_1 and SWS_2: wakefulness 11.0% to REM 22.0%, global mean 14.0%) and % source localization (Kruskal–Wallis p = .0266; range of two-way discordance means, proportion of spatial nonoverlap between SWS_1 and SWS_2: N2 24.6% to REM 41.0%, global mean 31.4%). Amongst n = 8 multifocal patients, N1 exhibited the most two-way discordance as a fraction of cortical grey matter (Kruskal–Wallis p = .0052; range of two-way discordance means, proportion of spatial nonoverlap between SWS_1 and SWS_2: N3 8.1% to N1 17.9%, global mean 12.0%), but when taken as % source localization, REM was most discordant (Kruskal–Wallis p = .0016; range of two-way discordance means, proportion of spatial nonoverlap between SWS_1 and SWS_2: N3 19.5% to REM 40.9%, global mean 30.6%). At spike take-off, SWS two-way discordances did not significantly differ for n = 8 unifocal patients as a fraction of cortical grey matter (Kruskal–Wallis p = .6824) nor of SWS source localization (Kruskal–Wallis p = .6790). For multifocal patients at spike take-off, SWS two-way discordances significantly differed such that REM exhibited the least discordance as a fraction of cortical grey matter (Kruskal–Wallis p = .0444; range of two-way discordance means, proportion of spatial nonoverlap between SWS_1 and SWS_2: REM 13.2% to NREM2 22.1%, global mean 18.4%), but the results were not significantly different as fractions of SWS source localizations (Kruskal–Wallis p = .6437).

REM disagrees with all other SWS to preferentially activate unique source voxels

At spike peak, REM was most likely of any SWS to localize to "unique" cortical grey matter voxels unoccupied by any of the other four SWS. Compared to the other four SWS, REM significantly revealed the greatest number of unique source activations, as a fraction of individualized cortical grey matter voxels (Kruskal–Wallis p = .0293; range of five-way discordance means, fraction of cortical grey matter: W 1.2% to REM 8.7%, global mean 3.6%; Figure 4C), and as a fraction of source localizations from a SWS (Kruskal–Wallis p = .0059; range of five-way discordance means, proportion of source localizations from a SWS that is unique: W 2.4% to REM 20.0%, global mean 8.6%; Figure 4D). At spike take-off, amount of unique source localization did not significantly differ as a fraction of a patient's total cortical grey matter voxels (Kruskal–Wallis p = .8560) nor as a fraction of that SWS source localization size (Kruskal–Wallis p = .8496).

Delineating unifocal and multifocal subgroups at spike peak, amongst n = 8 unifocal patients REM significantly revealed the greatest number of unique source activations, as a fraction of individualized cortical grey matter voxels (Kruskal–Wallis p = .0180; range of five-way discordance means, fraction of cortical grey matter: N2 0.6% to REM 11.4%, global

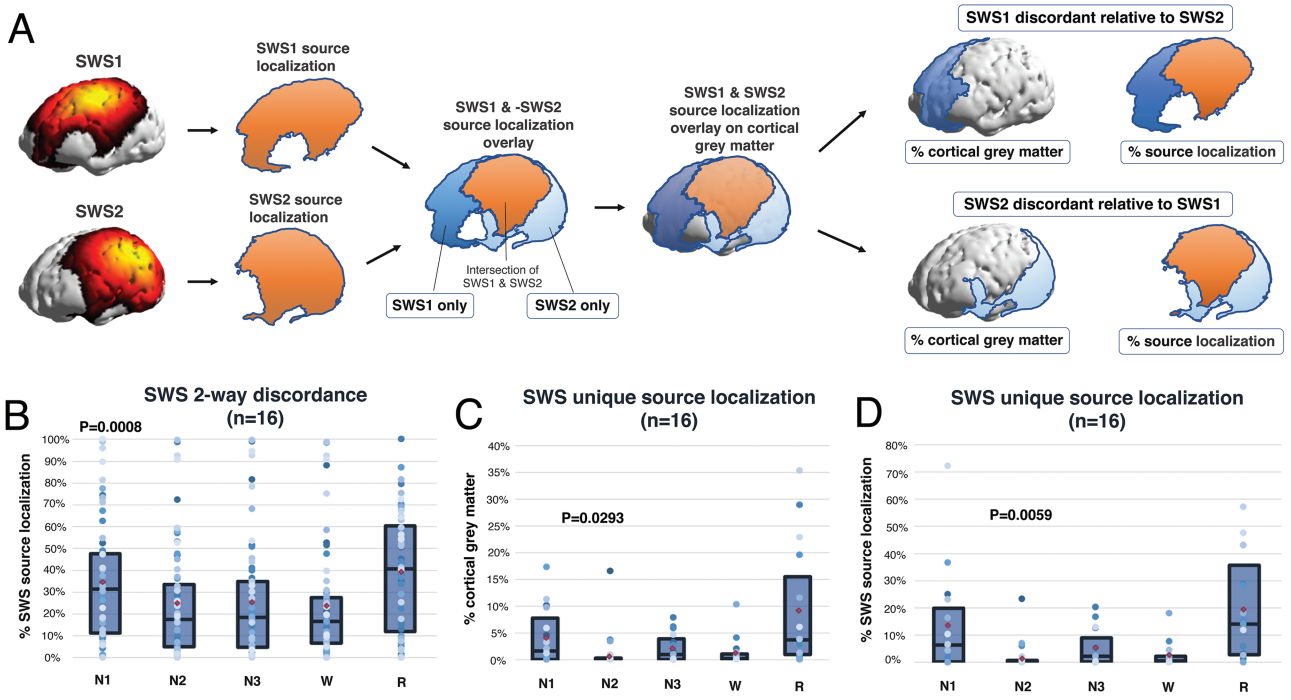

Figure 4. REM at spike peak preferentially activates unique source localizations. (A) Schematic illustrating discordance of source localizations for a hypothetical SWS_1 and SWS_2, expressed as a fraction of total cortical grey matter voxels in a given individual (left), and total source localizations for a given SWS (right). Diamonds depict the mean, dots depict individual patient data points, and boxes depict median ± IQR. (B) two-way discordances of each SWS, expressed as a fraction of SWS source localization size. Unique source localizations by each SWS expressed as a fraction of (C) total cortical grey matter, and (D) SWS source localizations.

mean 3.6%), and as a fraction of source localizations from a SWS (Kruskal–Wallis p = .0242; range of five-way discordance means, proportion of source localizations from a SWS that is unique: N2 1.0% to REM 19.9%, global mean 8.7%). Amongst n = 8 multifocal patients, amount of unique source localization revealed did not vary by SWS as a fraction of cortical grey matter (Kruskal–Wallis p = .5269), nor as a fraction of SWS source localizations (Kruskal–Wallis p = .3231). At spike take-off, SWS did not significantly differ in the amount of unique source localization for unifocal patients as a fraction of cortical grey matter (Kruskal–Wallis p = .9185) nor as a fraction of SWS source localization (Kruskal–Wallis p = .8518). Likewise in the multifocal subgroup at spike take-off, SWS did not significantly differ in the amount of unique source localization for unifocal patients as a fraction of cortical grey matter (Kruskal–Wallis p = .4723) nor as a fraction of SWS source localization (Kruskal–Wallis p = .6744).

Minimal effect of spike count

Because the vast majority of significant SWS differences were from spike peak analysis, we further analyzed the effect of spike count on spike peak analyses of SWS source localization size, concordance, and discordance. We found no significant correlation between the number of spikes in any SWS and source localization size (Supplementary Table S1). Similarly, there was no significant correlation between spike count and two-way concordance (Supplementary Table S2). Regarding two-way discordance (Supplementary Table S3), N1 and N3 exhibited low-to-moderate strength negative correlations with spike count (N1: Spearman's rho = –0.3797, Benjamini–Hochberg corrected p = .0145; N3 Spearman's rho = –0.4018, Benjamini–Hochberg corrected p = .0097). For each additional spike in N1 and N3, there was respectively mean 0.9% and 0.7% less two-way discordance (% cortical grey matter). Likewise, grouping all instances of SWS two-way discordance (N1, N2, N3, W, R), there was a low-to-moderate strength negative correlation with spike count such that, for each additional spike in an SWS, there was mean 0.5% less two-way discordance (Spearman's rho = –0.3043, Benjamini–Hochberg corrected p < .0001; % cortical grey matter). Regarding five-way discordance, there was no significant correlation with spike count for any individual SWS (Supplementary Table S4). However; grouping all instances of SWS five-way discordance (N1, N2, N3, W, R) there was a low-to-moderate strength negative correlation with spike count, such that, for each additional spike in an SWS, there was mean 0.3% less five-way discordance (Spearman's rho = –0.4408, Benjamini–Hochberg corrected p < .0001; % cortical grey matter).

Discussion

We used sLORETA to calculate which of the 256 652 individualized total cortical grey matter voxels from 16 prospectively recruited adult focal epilepsy patients demonstrated presence of a plausible source generator for 563 spikes from 80 SWS across patients. All patients had interictal spikes in all five canonical SWS, and spikes were analyzed at peak and take-off. This ESL strategy allowed us to generate an sLORETA model that tracks, voxel-by-voxel within individual brains of each patient, how SWS agreed and disagreed on the size and location of interictal spike source localizations.

SWS differences are apparent at spike peak rather than take-off

Source-localizing at spike peak, we found important differences between SWS in source localization size, concordance, and discordance. In contrast, there was only one statistically significant difference when source-localizing based on spike take-off. Of note, at spike take-off there was no significant difference between the source localization sizes of multifocal vs. unifocal patients. This is unexpected, because sLORETA incorporates multifocal spikes from different locations together into one overall source localization result. Thus, one would expect larger source spaces in multifocal than unifocal patients, which we observed at spike peak but not spike take-off. The inability to show this expected result at spike take-off suggests that, in our study, spike peak analysis was methodologically better positioned to detect SWS differences, assumedly due to the spike peak's superior signal-to-noise ratio [29, 36, 37] and visual reproducibility that enables standard inter-spike and inter-SWS comparisons.

Significant SWS differences at spike peak but not take-off further suggests that SWS ESL differences may incorporate the effects of intra-spike propogation. In contrast to *ictal* propagation, which occurs over seconds-to-minutes and may spread epileptic activity into very distant brain regions, *intra-spike* propagation occurs within milliseconds by definition, and expectedly remains confined in a single sublobar region [38]. Intra-spike propagation varies by individual, with certain spikes/patients exhibiting a minimal amount [38]. Intra-spike propagation can alter ESL results, though not always significantly [37]. Because of intra-spike propagation, it is controversially discussed whether spike peak, take-off, or mid-point ESL analyses best concur with epileptogenic zones [28, 29, 36–39]. By revealing significant SWS differences only at spike peak, our data suggest SWS electrodynamic mileux affect how spikes are expressed from the source generator. Although outside the scope of this present study, future work should consider tracking ESL differences within spikes over time—the resolution of which would be limited only by equipment sampling rate—to focus solely on intra-spike propagation differences between different SWS.

REM source localizations are smaller in multifocal than unifocal patients at spike peak

At spike peak, source localization size did not significantly vary between SWS, but interictal REM source localizations were significantly smaller amongst multifocal patients than unifocal patients. This suggests that, compared to other SWS at spike peak, REM sleep may "focalize" multifocal sources, pruning spurious estimations in multifocal patients that artificially cover greater brain space. We captured this effect at spike peak but not spike take-off, which may suggest differential intra-spike propagation as a mechanism, or could reflect the superior signal-to-noise ratio of spike peaks. Our finding of smaller multifocal REM source localizations agrees with previous works that note typically smaller epileptic phenomena in REM [12, 22, 40, 41]. However, only Kang et al. previously used ESL to compare the source localization size of REM versus NREM (an amalgam, excluding N1; wakefulness also excluded) [22]. Of note, of Kang et al.'s n = 6

study subject, at least $n = 2$ would be considered multifocal in our study. Generally, works indicating REM smallness have occurred in terms of interictal spike voltage fields, also excluded certain SWS (e.g. N1, wakefulness) [22, 40, 41], and/or considered REM against an amalgam "NREM" stage bundling any or all of N1, N2, and N3 [12, 22, 40, 41]. Notably, distinct NREM stages fundamentally differ in physiology and cortical electrodynamics. [42] Here, we delineate all five canonical SWS to resolve all inter-SWS comparisons, instead of comparing REM to a makeshift NREM amalgam or an incomplete SWS set. Moreover, whereas an interictal spike voltage field depicts passively recorded topographical EEG activity, a source localization is the active topographical summation of probabilistic candidate solutions to the inverse problem of where a spike ultimately originated from (the "source").

The reduction of REM source localization size specifically in multifocal patients may reflect specific REM's effects in a brain with multiple epileptic sources. In the literature, there are various reports of REM "selecting" a single culprit focus that, seemingly often, turns out to be correct [23]. Scarlatelli-Lima et al. studied 56 patients with medically-refractory mesial temporal lobe epilepsy and found that, of 12 patients with bilateral NREM spikes, only 5/12 had unilateral spikes in REM [43]. Furthermore, in four of five patients in whom REM lateralized spikes, the unilateral REM spikes concurred with an ipsilateral structural lesion on MRI. Malow et al. studied 21 patients with medically-refractory mesial temporal lobe epilepsy [44]. Amongst seven patients with REM spikes, only 1 had bilateral REM spikes, compared to 10 patients having bilateral NREM spikes. Malow and Aldrich reported a case of focal epilepsy secondary to a left mesial temporal glioma, in which NREM spikes localized bitemporally and ictal EEG showed independent bilateral ictal onset [45]. But, all REM spikes lateralized to the left temporal region (concordant with glioma). The glioma was resected and seizure freedom was achieved. Lieb et al. studied spikes on intracranial depth recording for nine medically refractory temporal lobe epilepsy patients who underwent surgical resection [46]. In seven patients, REM lateralized to the hemisphere of resection and concurred with the hemisphere of resection more than any other SWS, with 4/7 REM lateralized patients having Engel I outcome. These reports suggest that when an apparent spike onset zone is diferentially well-expressed in REM, it is more likely concordant with a true epileptogenic zone.

With regard to relatively larger REM source localizations in unifocal patients, there have been reports of interictal REM epileptic phenomena covering novel brain regions [22, 23, 47–49]. However, this has never been studied in a systematic, quantitative fashion. Although our unifocal REM findings were relative, it is still worth emphasizing that even an absolutely larger spatial extent of estimated source localizations does not necessarily translate into an actual larger source generator; rather, there may simply be more candidate source solutions over greater brain space. This is especially true at spike peak, after which intra-spike propagation may have occurred. Another consideration is that greater degrees of freedom in ESL source space set a higher bar for "correct localization", and increase the possibility of SWS disagreement. Voltage fields sharing the same localization in so-called "sensor space" (for example, two spikes with a maximum field at the T3 electrode) may markedly differ from one another when subject to ESL in the much vaster space of thousands of cortical voxel parcellations over individualized neuroanatomical co-localizations. Notably, without ESL, even intracranial EEG remains a passive depiction of interictal spike electrical fields, albeit closer to the presumed source. Although we were limited by small numbers (eight unifocal and multifocal patients each), these data suggest that REM spike source localization effects can differ when applied to single or multiple epileptic foci, especially when incorporating the effects of intraspike propagation.

SWS redistribute source localizations throughout cortex, but retain an omniconcordant "core"

Within all patients, irrespective of unifocality or multifocality, interictal source localizations from the five SWS on spike peak and take-off analyses convergently localized to a shared region spanning about 20% of total cortical grey matter on average. This "omniconcordant" region roughly involved a mean of 45% of the source localizations from each SWS, with SWS not significantly differing from one another. Beyond this five-way omniconcordant SWS "core", both spike peak and take-off analyses showed a further "penumbra" of two-way SWS concordances involving on average 10%–35% more source localizations from each SWS. This is equivalent to a mean total of 55%–80% of the source localizations from any given SWS being spatially concordant with at least 1 other SWS. Unlike five-way omniconcordance, two-way concordances significantly differed between SWS at spike peak. Notably, REM was least two-way concordant, while not significantly detracting from omniconcordance. Compared to other SWS, these findings suggest an effect where REM redistributes source localizations by selectively "moving" them away from shared cortical grey matter voxels activated by any 1 other SWS (i.e. the concordant penumbra), but not away from those shared with all four other SWS at the same time (i.e. the omniconcordant core). Because spike peak analysis can incorporate an element of intraspike propagation, this "movement" of source localization voxels may reflect REMs unique electrodynamic mileux exerting a unique effect on how spikes are expressed from their source generator.

REM preferentially activates unique epileptic source localizations at spike peak

REM is not only is the least agreeable SWS at spike peak but also the most spatially disagreeable in terms of activating new interictal source localizations relative to other SWS. Whereas a mean of 20%–30% of source localizations from other SWS disagreed with any 1 other SWS at spike peak, REM was proportionally most two-way discordant, with 40% of its source localizations disagreeing with any 1 other SWS on average. Like two-way concordances, there was no significant difference between SWS when two-way discordance was taken as a fraction of all individualized cortical grey matter voxels of the entire brain, but REM was significantly most two-way discordant at spike peak as a fraction of SWS source localization voxels. These findings support the suggestion that, at spike peak compared to other SWS, REM redistributes source voxels away from the aforementioned two-way concordant penumbra, which is then captured in overall enhanced two-way discordance. As with our concordance findings, REMs difference from other SWS may relate to an intra-spike propagation-related effect.

Though limited by small sample size, our unifocal vs. multifocal subgroup analysis suggests that REM two-way discordance is more pronounced among unifocal than multifocal epilepsy patients. Among multifocal patients at spike peak, REM was most two-way discordant as a fraction of SWS source localization size, but N1 was most two-way discordant in terms of cortical grey matter. N1 discordance could be a topic of future study. These findings also suggest that relatively small REM source localizations at spike peak amongst multifocal patients contain a proportionally high degree of two-way discordance. More strikingly, REM reveals more truly unique interictal source localizations than any other SWS; a clear SWS effect. Defining REMs novelty as unique voxels activated only by REM and none of the four other SWS, REMs novelty at spike peak was more than twice that of N1, the next-most-novel SWS. Roughly 20% of REMs source localizations were in unique voxels unactivated by any other SWS (corresponding to mean 8.7% individualized cortical grey matter voxels).

Clinical and mechanistic implications of REM source localizations

An important consideration is that the spatial extent of interictal source localizations within the brain is not the same as the physical extent of the epileptic source generator itself. Rather, source localizations are calculated estimates and sLORETA had used individualized cortical grey matter voxels as the "unit" of source localization. Although physical epileptic generators (and their networks) do not necessarily follow voxel dimensions, by holding constant both physical generators and calculated voxels within each patient, we were able to fairly compare the relative effects of different SWS on personalized localization estimates of the same source generator.

At spike take-off and peak, we found a substantial omniconcordant core within patients that anchored interictal source localizations between SWS to confirm presence of the same source generator. This was a necessary confirmation of internal validity, and prerequisite to further analyses. However, the relative localizing values of different SWS only manifest in differential localizations beyond the omniconcordant core, i.e. where there is some disagreement. REM sleep is, notably, the SWS bearing most evidence of superior localizing abilities [12, 15, 22, 41, 46, 47, 50, 51]. Intruigingly, in our study, REM is the SWS with the most differential effects on source localization. Most notably, REM source localizations activate unique cortical voxels, untouched by the source localizations of any other SWS. Validation with resective surgery, leading to seizure freedom, would be necessary to confirm the clinical utility of these unique source activations. It could be that REMs superior localizing abilities are due to an ability to find candidate sources that no other SWS can—but are in fact correct. Our recent literature review found that when REM disagreed with all other SWS to provide a unique localization, this novel localization has been empirically correct, per the gold standard of seizure freedom postresective surgery [23]. On the contrary, whenever REMs localization was incorrect (as per continuation of seizures postsurgery), REM has not been uniquely "wrong", having been accompanied by ≥1 other SWS. This suggests the possibility for REM source localizations to disagree with other SWS, and be correct.

REMs unique source activation ability at spike peak may reflect an intraspike propagation tendency that is different from other SWS. Mechanistically, this may relate to REMs asynchrony. While REM asynchrony may destructively interfere with intraspike propagation, spatially constraining the discharge and enhancing localization specificity [52, 53], it is also conceivable that constructive interference may propagate epileptic activity in novel brain cortex otherwise constrained by other SWS. This is also made more plausible by unusual cortico-cortical connections described in REM, and a REM shift toward "larger-world" functional networks [54, 55]. This hypothetical mechanism could also partially explain why seizures and spikes are comparatively rare in REM, with spikes breaking through REM often diminutive and blunt: [44, 56–58] altered cortico-cortical connections, and greater asynchrony with constructive interference, may reduce the ability for spike and seizure formation due lack of local synchronous current needed for ictogenesis. Future study could aim to characterize such effects closer to spike onset, such as whether REM promotes atypical coalesnce patterns of putative epileptic "microdomains", characterized on human intracranial microelectrode EEG [48, 49].

Limitations

Given the preeminence of REM in our findings, a study limitation is lack of chin electromyography to reliably indicate muscle atonia, which may have increased the difficulty of identifying REM, especially for short transitionary periods or longer epochs of tonic REM lacking the eye movements of phasic REM. Although surface EEG is standard for sleep scoring, this study was limited by not incorporating intracranial EEG. While intracranial EEG is anatomically closer to the presumed true source of epileptic activity, implantation and recording strategies are nevertheless inherently idiosyncratic to a given patient, sampling small amounts of cortex and greatly precluding fair concordance and discordance comparisons by SWS between subjects. In contrast, we selected spike peak and take-off as recorded on standard surface 10–20 electrode configuration (with consistent additional subtemporal chains) for ESL, to fairly compare SWS against one other at different points of intraspike signal spread.

This study was also limited by using standard-density rather than high-density EEG, with the latter having greater reported ESL accuracy [59]. It is possible that a similar future study using high-density EEG may generate discordant findings. However, standard density EEG has been shown to approach 90% accuracy as confirmed by postsurgical seizure freedom [18], and 80% accuracy in MRI-negative cases [19]. Other recent work found sLORETA based on standard density EEG is equally accurate as connectivity measures to localize the EZ [20]. Therefore, our methodology is appropriate to characterize certain SWS effects upon spike source localization. However, we may have been limited in our ability to detect SWS effects at spike take-off, where the signal-to-noise ratio is lower [29, 36, 37].

We used sLORETA because it has zero systematic localization error compared to other LORETA ESL methods [32], and it can distinguish and construct multiple sources simultaneously, including unconnected shallow and deep grey matter arrays that would have been surveyed intracranially. However, less synchronized background brain oscillations during REM may impact the accuracy of a method such as sLORETA when compared to other ESL methods. Therefore, future work should also consider reproducing SWS concordance and discordance effects using as many

different ESL methods as possible [32, 33]. For example, maximum entropy on the mean (MEM) is another widely used ESL method in epilepsy that has been validated as showing congruence with clinical seizure onset zones [22, 60]. Within sLORETA, we applied a standard threshold to individualized cortical grey matter voxels to establish spatial extents of source localizations. Future studies may consider other nonstandard customized thresholds, or unthresholded data for weighted spatial analyses.

Spikes in this study were collected from routine clinical care. Inevitably, patients exhibited different amounts of spikes in different SWS. We found that source localization size and concordance did not correlate with SWS spike count, but two-way and five-way discordance results showed weak-to-moderate negative correlations with spike count, when pooling the data for all SWS (N1, N2, N3, W, R). The only individual SWS results exhibiting correlations to spike count were N1 and N3 two-way discordance (also weak-to-moderate negative correlations). Nonetheless, REM having fewer spikes may have exaggerated its discordance findings by a low-to-moderate amount. Spikes in REM are known to be rare; certain patients will simply not exhibit frequent spikes in all states of vigilance [58], either for a neurobiological reason [53] or simply due to not enough day–nights recorded. We opted to include patients with low spike counts, as has been done in other work applying source localization to spikes in different SWS [22]. Ideally, a robust spike count in each SWS should be captured and analyzed, with future work looking into what is an optimal number. This may be fostered by using automated methods to exhaustively capture all spikes that a patient exhibits [61]. Automatic spike collection could also be applied to exhaustively multifocal patients to compare multiple spike populations against one another, in as many SWS as they occur. Another consideration for multifocal patients would be to isolate one dominant spike type and characterize its spatial fluctuations across sleep–wake states, whereas in the present work we compared SWS based on the totality of the spikes they exhibited.

Another clinical consideration is that the majority of our patients (11/16) had temporal lobe epilepsy. Future work may focus on extratemporal patients with more spatially complex epilepsies that require extensive presurgical workup, because these patients may be more likely to benefit from ESL techniques. While ESL accuracy in our study benefitted from personalized brain models for the majority of patients (12/16), standardized cortex templates had to be used in a few, including one patient with remote prior left temporal lobectomy, and no recent clinical MRI available for individualized brain modeling. Use of a standard template likely limits the ground-truth accuracy of source localization. However, our dataset does not allow us to validate particular SWS as succeeding or failing to localize a ground truth EZ as confirmed by postresective seizure freedom—nor was this our goal. Rather, we sought to compare SWS source localization size, spatial overlap, and spatial nonoverlap, at spike peak and take-off. As long as the same cortex is used within an individual, we believe this should be a reasonable "level playing field" within which all resultant estimated source localizations can be mapped for fair inter-SWS comparison.

Nonetheless, SWS concordance with the ground-truth epileptogenic zone as validated by postresective surgery seizure freedom would be the most impactful clinical comparator. Only 2 of 16 patients had *bona fide* resective surgery, but they continued to have seizures post-operatively such that the epileptogenic zone was incompletely removed. In our present cohort, postsurgical data are limited but supports REM as the best localizing SWS. Specifically, patient 2 received epilepsy surgery after the EMU admission in which our study data were gathered, undergoing repeat resection of residual left posterior insular cavernoma. Although complete resection was not possible to avoid neurological deficit, he experienced a dramatic reduction in right hemisensory seizures (Engel II). Composite spikes from each SWS included the to-be resected left posterior insular region, but REM yielded the smallest source localization, triangulating the insula with greatest specificity among SWS (Supplementary Figure S1). Future work could compare different SWS, and their shared omniconcordant zone, against ground truth epileptogenic zones.

Conclusion

In our cohort of prospectively recruited patients with focal epilepsy, REM was best suited of all SWS to identify candidate epileptic sources. We used sLORETA to develop a model using an intraindividual voxel-by-voxel approach to ESL of the interictal spike source generator, and applied this model to SWS spikes at peak and take-off. We found a core region of source localizations shared by all five canonical SWS. This "omniconcordant core" is surrounded by a "penumbra" of less concordant and more discordant source localizations between just two SWS. Out of all SWS, REM spares the omniconcordant core to draw on the concordant penumbra for source voxels located in unique cortex that no other SWS can find. Based on spike peak analysis, REM shrinks source localization size preferentially in patients with multifocal epilepsy. While these findings may reflect differential intraspike propagation in REM, they require further study. These findings extend present knowledge of the profound impacts of sleep on localization in epilepsy and provide a possible model accounting for REMs reportedly superior localizing ability out of all SWS.

Supplementary Material

Supplementary material is available at *SLEEP* online.

Acknowledgments

We gratefully acknowledge the contributions of posthumous Amirhossein Ghassemi, who tragically passed away aboard Ukraine International Airlines Flight 752 before this manuscript was completed.

Funding

This work was supported by funding from The Canadian Institutes of Health Research, Mathematics of Information Technology and Complex Systems Accelerate Grant (Grant no. IT15617), and the Health Sciences Centre Foundation.

Disclosure Statement

Financial disclosure: none.

Non-financial disclosure: none.

Data Availability Statement

The data underlying this article will be shared on reasonable request to the corresponding author.

References

1. England MJ, Liverman CT, Schultz AM, Strawbridge LM. *Epilepsy across the spectrum: Promoting health and understanding. Epilepsy Across the Spectrum: Promoting Health and Understanding*. Washington D.C.: National Academies Press, 2012. doi:10.17226/13379
2. Beghi, E. *et al*. Global, regional, and national burden of epilepsy, 1990–2016: a systematic analysis for the Global Burden of Disease Study 2016. *Lancet Neurol*. 2019;**18**:357–375.
3. Devinsky O, *et al*. Recognizing and preventing epilepsy-related mortality: a call for action. *Neurology*. 2016;**86**(8):779–786.
4. Bell B, *et al*. The neurobiology of cognitive disorders in temporal lobe epilepsy. *Nat Rev Neurol*. 2011;**7**(3):154–164.
5. Kwan P, *et al*. The natural history of epilepsy: An epidemioloqical view. *J Neurol Neurosur Psychiatry*. 2004;**75**:1376–1381.
6. Kwan P, *et al*. Early identification of refractory epilepsy. *N Engl J Med*. 2000;**342**(5):314–319.
7. de Tisi J, *et al*. The long-term outcome of adult epilepsy surgery, patterns of seizure remission, and relapse: a cohort study. *Lancet*. 2011;**378**(9800):1388–1395.
8. Picot MC, *et al*. Cost-effectiveness analysis of epilepsy surgery in a controlled cohort of adult patients with intractable partial epilepsy: a 5-year follow-up study. *Epilepsia*. 2016;**57**(10):1669–1679.
9. Jin P, *et al*. Towards precision medicine in epilepsy surgery. *Ann Transl Med*. 2016;**4**(2):24.
10. Malmgren K, *et al*. Long-term outcomes of surgical treatment for epilepsy in adults with regard to seizures, antiepileptic drug treatment and employment. *Seizure*. 2017;**44**:217–224.
11. Klimes P, *et al*. NREM sleep is the state of vigilance that best identifies the epileptogenic zone in the interictal electroencephalogram. *Epilepsia*. 2019;**60**(12):2404–2415.
12. Okanari K, *et al*. Rapid eye movement sleep reveals epileptogenic spikes for resective surgery in children with generalized interictal discharges. *Epilepsia*. 2015;**56**(9):1445–1453.
13. Bagshaw AP, *et al*. Effect of sleep stage on interictal high-frequency oscillations recorded from depth macroelectrodes in patients with focal epilepsy. *Epilepsia*. 2009;**50**(4):617–628.
14. Ochi A, *et al*. Lateralized interictal epileptiform discharges during rapid eye movement sleep correlate with epileptogenic hemisphere in children with intractable epilepsy secondary to tuberous sclerosis complex. *Epilepsia*. 2011;**52**(11):1986–1994.
15. Sakuraba R, *et al*. High frequency oscillations are less frequent but more specific to epileptogenicity during rapid eye movement sleep. *Clin Neurophysiol*. 2016;**127**(1):179–186.
16. Michel CM, *et al*. EEG mapping and source imaging. In Schomer DL. Lopes da Silva FH., eds. *EEG Mapping and Source Imaging*, vol. **1** Oxford University Press; 2017.
17. Michel CM, *et al*. EEG source imaging: a practical review of the analysis steps. *Front Neurol*. 2019;**10**:325.
18. Sperli F, *et al*. EEG source imaging in pediatric epilepsy surgery: a new perspective in presurgical workup. *Epilepsia*. 2006;**47**(6):981–990.
19. Russo A, *et al*. The diagnostic utility of 3D electroencephalography source imaging in pediatric epilepsy surgery. *Epilepsia*. 2016;**57**(1):24–31.
20. Coito A, *et al*. Interictal epileptogenic zone localization in patients with focal epilepsy using electric source imaging and directed functional connectivity from low-density EEG. *Epilepsia Open*. 2019;**4**(2):281–292.
21. Gibbs E, *et al*. Diagnostic and localizing value of electroencephalographic studies in sleep. *J Nerv Ment Dis*. 1947;**26**:336–376.
22. Kang X, *et al*. Quantitative spatio-temporal characterization of epileptic spikes using high density EEG: differences between NREM sleep and REM sleep. *Sci Rep*. 2020;**10**(1):1673.
23. McLeod GA, *et al*. Can REM sleep localize the epileptogenic zone? A systematic review and analysis. *Front Neurol*. 2020;**11**:584.
24. Fuchs M, *et al*. A standardized boundary element method volume conductor model. *Clin Neurophysiol*. 2002;**113**(5):702–712.
25. Céspedes-Villar Y, *et al*. Influence of patient-specific head modeling on EEG source imaging. *Comput Math Methods Med*. 2020;**2020**:5076865.
26. Bénar CG, *et al*. Modeling of post-surgical brain and skull defects in the EEG inverse problem with the boundary element method. *Clin Neurophysiol*. 2002;**113**(1):48–56.
27. Kural MA, *et al*. Criteria for defining interictal epileptiform discharges in EEG: a clinical validation study. *Neurology*. 2020;**94**(20):e2139–e2147.
28. Plummer C, *et al*. Interictal and ictal source localization for epilepsy surgery using high-density EEG with MEG: a prospective long-term study. *Brain*. 2019;**142**(4):932–951.
29. Ray A, *et al*. Localizing value of scalp EEG spikes: a simultaneous scalp and intracranial study. *Clin Neurophysiol*. 2007;**118**(1):69–79.
30. Wagner M, *et al*. Evaluation of sLORETA in the presence of noise and multiple sources. *Brain Topogr*. 2004;**16**(4):277–280.
31. Cox BC, *et al*. EEG source imaging concordance with intracranial EEG and epileptologist review in focal epilepsy. *Brain Commun*. 2021;**3**(4):fcab278.
32. Pascual-Marqui RD. Standardized low resolution brain electromagnetic tomography. *Methods Find Exp Clin Pharmacol*. 2002;5–12.
33. Cosandier-Rimélé D, *et al*. A realistic multimodal modeling approach for the evaluation of distributed source analysis: application to sLORETA. *J Neural Eng*. 2017;**14**(5):056008.
34. Plummer C, *et al*. Dipole versus distributed EEG source localization for single versus averaged spikes in focal epilepsy. *J Clin Neurophysiol*. 2010;**27**(3):141–162.
35. Jaccard P. Distribution de la flore alpine dans le bassin des Dranses et dans quelques régions voisines. *Bull Socieacuteteacute Vaudoise Sci Nat*. 1901;**37**.
36. Wang G, *et al*. Interictal spike analysis of high density EEG in patients with partial epilepsy. *Clin Neurophysiol Off J Int Fed Clin Neurophysiol*. 2011;**122**:1098–1105.
37. Vorderwülbecke BJ, *et al*. Automated interictal source localisation based on high-density EEG. *Seizure*. 2021;**92**:244–251.
38. Mălîia MD, *et al*. Epileptiform discharge propagation: analyzing spikes from the onset to the peak. *Clin Neurophysiol*. 2016;**127**(4):2127–2133.
39. Lantz G. *et al*. Propagation of interictal epileptiform activity can lead to erroneous source localizations: A 128-channel EEG mapping study. *J Clin Neurophysiol*. 2003;**20**:311–319.

40. von Ellenrieder N, *et al*. Physiological and pathological high-frequency oscillations have distinct sleep-homeostatic properties. *Neuroimage Clin*. 2017;**14**:566–573.
41. Ng MC. Maximizing the yield of rapid eye movement sleep in the epilepsy monitoring unit. *J Clin Neurophysiol*. 2017;**34**:61–64.
42. Carley DW, *et al*. Physiology of Sleep. *Diabetes Spectr*. 2016;**29**(1):5–9.
43. Scarlatelli-Lima AV, *et al*. How do people with drug-resistant mesial temporal lobe epilepsy sleep? A clinical and video-EEG with EOG and submental EMG for sleep staging study. *eNeurologicalSci*. 2016;**4**:34–41.
44. Malow BA, *et al*. Interictal spiking increases with sleep depth in temporal lobe epilepsy. *Epilepsia*. 1998;**39**(12):1309–1316.
45. Malow BA, *et al*. Localizing value of rapid eye movement sleep in temporal lobe epilepsy. *Sleep Med*. 2000;**1**(1):57–60.
46. Lieb JP, *et al*. Sleep state and seizure foci related to depth spike activity in patients with temporal lobe epilepsy. *Electroencephalogr Clin Neurophysiol*. 1980;**49**(5-6):538–557.
47. Mayersdorf A, *et al*. Focal epileptic discharges during all night sleep studies. *Clin Electroencephalogr*. 1974;**5**;73–87.
48. Watanabe Y, *et al*. Cluster of epileptic spasms preceded by focal seizures observed in localization-related epilepsy. *Brain Dev*. 2007;**29**(9):571–576.
49. Genton P, *et al*. Continuous focal spikes during REM sleep in a case of acquired aphasia (Landau-Kleffner syndrome). *Sleep*. 1992;**15**(5):454–460.
50. Yuan X, Sun M. The value of rapid eye movement sleep in the localization of epileptogenic foci for patients with focal epilepsy. *Seizure*. 2020 doi:10.1016/j.seizure.2020.06.009
51. Montplaisir J, *et al*. Nocturnal sleep recording in partial epilepsy: a study with depth electrodes. *J Clin Neurophysiol*. 1987;**4**(4):383–388.
52. Shouse MN, *et al*. Physiological basis: how NREM sleep components can promote and REM sleep components can suppress seizure discharge propagation. *Clin Neurophysiol*. 2000;**111 Suppl 2**:S9–S18.
53. Ng MC. Orexin and epilepsy: potential role of REM Sleep. *Sleep*. 2017;**40**.
54. Hein M, *et al*. The sleep network organization during slow-wave sleep is more stable with age and has small-world characteristics more marked than during REM sleep in healthy men. *Neurosci Res*. 2019;**145**:30–38.
55. Chow HM, *et al*. Rhythmic alternating patterns of brain activity distinguish rapid eye movement sleep from other states of consciousness. *Proc Natl Acad Sci U S A*. 2013;**110**(25):10300–10305.
56. Sammaritano M, *et al*. Interictal spiking during wakefulness and sleep and the localization of foci in temporal lobe epilepsy. *Neurology*. 1991;**41**(2 (Pt 1)):290–297.
57. Frost JD Jr, *et al*. Sleep modulation of interictal spike configuration in untreated children with partial seizures. *Epilepsia*. 1991;**32**(3):341–346.
58. Ng M, *et al*. Why are seizures rare in rapid eye movement sleep? Review of the frequency of seizures in different sleep stages. *Epilepsy Res Treat*. 2013;**2013**:932790.
59. Brodbeck V, *et al*. Electroencephalographic source imaging: a prospective study of 152 operated epileptic patients. *Brain*. 2011;**134**(Pt 10):2887–2897.
60. Pellegrino G, *et al*. Source localization of the seizure onset zone from ictal EEG/MEG data. *Hum Brain Mapp*. 2016;**37**(7):2528–2546.
61. Jing J. *et al*. Development of expert-level automated detection of epileptiform discharges during electroencephalogram interpretation. *JAMA Neurol*. 2020;**77**:103–108.